eng

MDPI

Article

An Investigation of Increased Power Transmission Capabilities of Elastic–Plastic-Designed Press–Fit Connections Using a Detachable Joining Device

Jan Falter *, Daniel Herburger, Hansgeorg Binz and Matthias Kreimeyer

Institute for Engineering Design and Industrial Design (IKTD), University of Stuttgart, Pfaffenwaldring 9, 70569 Stuttgart, Germany; hansgeorg.binz@iktd.uni-stuttgart.de (H.B.); matthias.kreimeyer@iktd.uni-stuttgart.de (M.K.)

* Correspondence: jan.falter@iktd.uni-stuttgart.de

Abstract: Drive systems are an important part of general mechanical engineering, automotive engineering, and various other fields, with shaft–hub connections being an important part of such systems. Decisive aspects in the development of such systems today are, for example, high transmittable forces and torques, low masses, and the cheapest possible production of components. A possibly threefold increase in the force and torque transmission capacity can be achieved by using press–fit connections with an elastic–plastic design as opposed to regular elastically designed alternatives. An elastic–plastic design of the press–fit connection is achieved by using a large interference. A large transition geometry on the shaft (which replaces the conventional chamfer) is required to join such an interference. The material and space requirements have a negative impact on lightweight applications and limited building spaces. Therefore, the objective of the research presented in this paper is to design and analyze a detachable joining device that substitutes this geometry. A simulation study was conducted to determine the geometry of the joining device that improves the stress state and consequently the force and torque transmission capacity of the connection. Moreover, the influence of manufacturing tolerances of the joining device and the shaft, corresponding risks, and measures to mitigate them are analyzed using finite element analysis. The results show that large transition radii, enabled by using a joining device, lead to a homogenous distribution of plastic strain and pressure in the press–fit connection, even for large interferences ξ and soft hub materials like wrought aluminum alloys. The influence of manufacturing tolerances on the stress state was quantified, leading to design guidelines that minimize the risk of, e.g., the front face collision of a shaft and hub, while maximizing the power transmission of the connection. The results show the capability of a detachable joining device to enable elastic–plastic press–fit connections and the corresponding threefold increase in the force and torque transmission capacity in lightweight applications, resulting from the substitution of the installation space consuming and mass increasing the transition geometry of the shaft.

Keywords: elastic–plastic design; finite element analysis; interference fit; joining device; power transmission; shaft–hub connection

Citation: Falter, J.; Herburger, D.; Binz, H.; Kreimeyer, M. An Investigation of Increased Power Transmission Capabilities of Elastic–Plastic-Designed Press–Fit Connections Using a Detachable Joining Device. *Eng* **2024**, *5*, 1155–1172. https://doi.org/10.3390/eng5030063

Academic Editor: Antonio Gil Bravo

Received: 22 April 2024
Revised: 17 June 2024
Accepted: 18 June 2024
Published: 21 June 2024

1. Introduction

A primary objective in the development of drive systems is to increase the power density and to reduce the installation space and mass [1]. A crucial component to accomplish this goal is enhancing the force and torque transmission capacity of shaft–hub connections. A particularly important representative of these connections is the interference–fit connection, as it is characterized by its cost-effective production [1–4] and ability to transmit alternating forces and moments [5]. One effective way to increase the transmission capacity of interference–fit connections is to augment the diametral interference between the hub and shaft [3,6]. This is in engineering practice often restricted by the elastic limit of the used material, limiting the interference to approximately 1–2‰. However, a threefold increase in

the transmission capacity is achievable by allowing for the plastic deformation of the hub as part of an elastic–plastic design, using interferences up to 100‰ [7,8]. Due to the large interference, however, such press–fit connections cannot be joined using thermal expansion (shrink–fit connection), as this would require exceeding the annealing temperatures of the hub materials. It is therefore necessary to press the shaft into the bore of the hub (press–fit connection), e.g., by using a hydraulic press. This joining process is subject to extensive requirements due to its influence on the transmission capacity of the press–fit connection. Previous research [8] indicates that in order to achieve a stress state of the connection that allows for an increase in the transmission capacity, a specific transition radius between the shaft's cylindrical contact area and the end of the shaft is necessary.

This research article studies the potential of using a detachable joining device (JD) as a substitute for the shaft's transition radius to decrease weight, material consumption, and installation space while increasing the force and torque transmission capacity. Moreover, this research article examines the challenges of such a device related to manufacturing tolerances and corresponding corrective actions. Finite element simulations are used to find a suitable transition radius and to determine the influence of manufacturing tolerances on the pressure distribution and strains in the hub. Based upon this, a design recommendation for a joining device that is suitable for elastic–plastic-designed press–fit connections is presented.

1.1. Research Problem

Augmenting the diametral interference and therefore the transmission capacity of elastic–plastic-designed press–fit connections results in increasing the complexity of its prevailing triaxial stress condition [8]. Most importantly, the pressure between the shaft and hub, corresponding to the radial stress within the interface, becomes more inhomogeneous with rising diametral interferences. For larger interferences, an increasingly significant drop in the radial stress occurs within the interface in the region of the axial hub center, which is—according to [8]—related to increased local plastic strain. Consequently, this pressure reduction leads to a decreased transmission capacity of the press–fit connection. Moreover, the risk of failure due to fretting fatigue increases for connections with a locally decreased pressure that are subjected to dynamic torsional and bending moments. Increasing the transition radius leads to an increase in pressure within the axial hub center of elastic–plastic-designed press–fit connections. However, within prior research [7,8], it had to be considered that an augmented transition radius leads to an increase in mass and installation space for the shaft [8].

1.2. Research Objective

As described above, the elastic–plastic design requires a large transition radius to achieve a uniform pressure distribution without a strong decrease in the center of the hub. Only then will the average pressure in the interface between the shaft and hub be high, leading to an increased ability to transmit forces and torques. However, a large transition radius causes the shaft to grow in the axial direction and introduces undesired mass into the technical system.

Therefore, the main objective of this article is to apply the elastic–plastic design in such a way that high and uniform pressures are achieved between the hub and the shaft.

In addition, this article pursues the secondary objective of designing the geometry of the component required for the main objective to be as small and light as possible in order to meet the requirements of lightweight applications, which are becoming increasingly important.

By fulfilling these objectives, for the first time, a significantly increased force and torque transmission capacity, a small installation space, and a low mass of elastic–plastic-designed press–fit connections can be achieved simultaneously. The power density can thus be increased threefold [8], which opens up the use of press–fit connections in applications

that were previously restricted to more expensive and complex positive-fit shaft–hub connections.

1.3. Research Approach

To achieve the described objectives, it is proposed to use a detachable joining device, broadening the design flexibility substantially. With this, it will be possible to separate the necessary but disadvantageously large and heavy geometry of the transition radius from the press–fit connection. Finding the best possible geometry for the joining device, a first series of simulations is utilized to identify the relation between large transition radii and the homogeneity of the plastic strain distribution in the connection. For this simulation series, an initial examination of the aforementioned relation between the transition radius and the pressure distribution by Kröger et al. [7] is adopted and the examination space considerably increased. The obtained results serve as a quantified measure for the potential of large transition radii to increase the transmission capacity of press–fit connections and consequently the potential of the joining device as the enabler for their application (cf., Section 4.1). As a result, the most suitable transition radius will be found to meet the objective of a high and homogeneous pressure distribution, leading to an increased force and torque transmission capacity.

The potential of the detachable joining device to improve the stress state of the connection while decreasing the mass and installation space of the shaft relies on the feasibility of the transition of the hub from the joining device to the shaft. Consequently, a second series of simulations is used to investigate the influence of the junction geometry (shown in Figures 1 and 2) on the transmission capacity of the press–fit connection (cf., Section 4.2). Moreover, the effects of manufacturing tolerances in the junction region (cf., Figure 1) and resulting process risks are investigated (cf., Section 4.3). For this purpose, various achievable tolerance ranges are examined in finite element simulations. The objective of this set of iterative numerical investigations is to achieve the highest possible and most uniform pressure distribution in the interface between the shaft and hub.

The numerical simulations are built upon the investigations presented in [8]. The adopted experimentally validated elastic–plastic material model is described in Section 3.1. The definition of the finite element model used is given in Section 3.2. A validation of the numerical simulations of the joining process of the press–fit connections using the detachable joining device is given by experimental data in Section 4.4.

Subsequently, the results are discussed and a design recommendation for the joining device is derived and presented in Section 5. The research article is then closed by a general conclusion in Section 6.

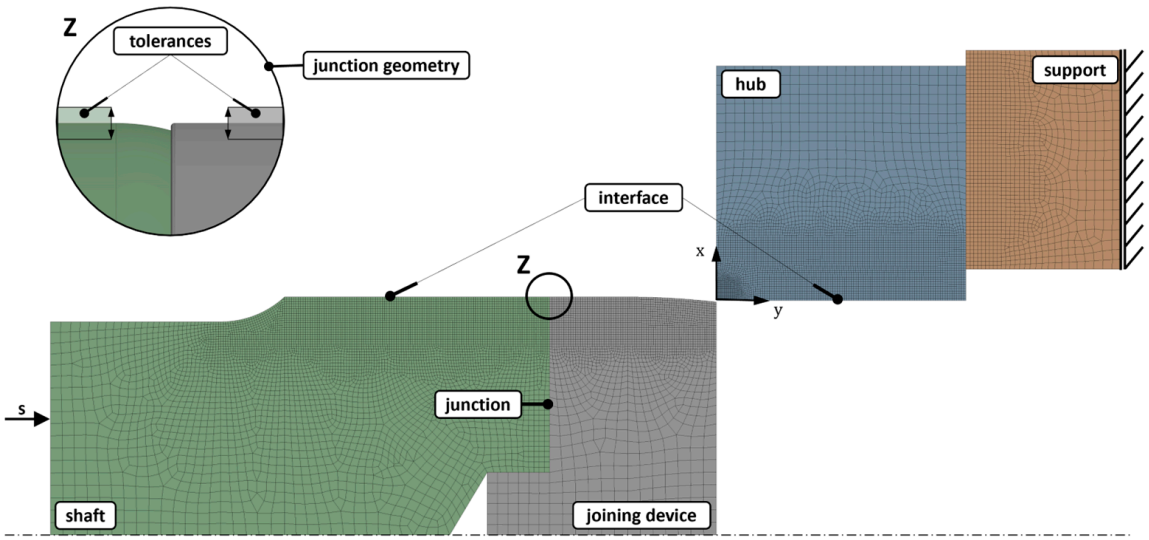

Figure 1. Geometry of the simulation model with detail Z (junction geometry).

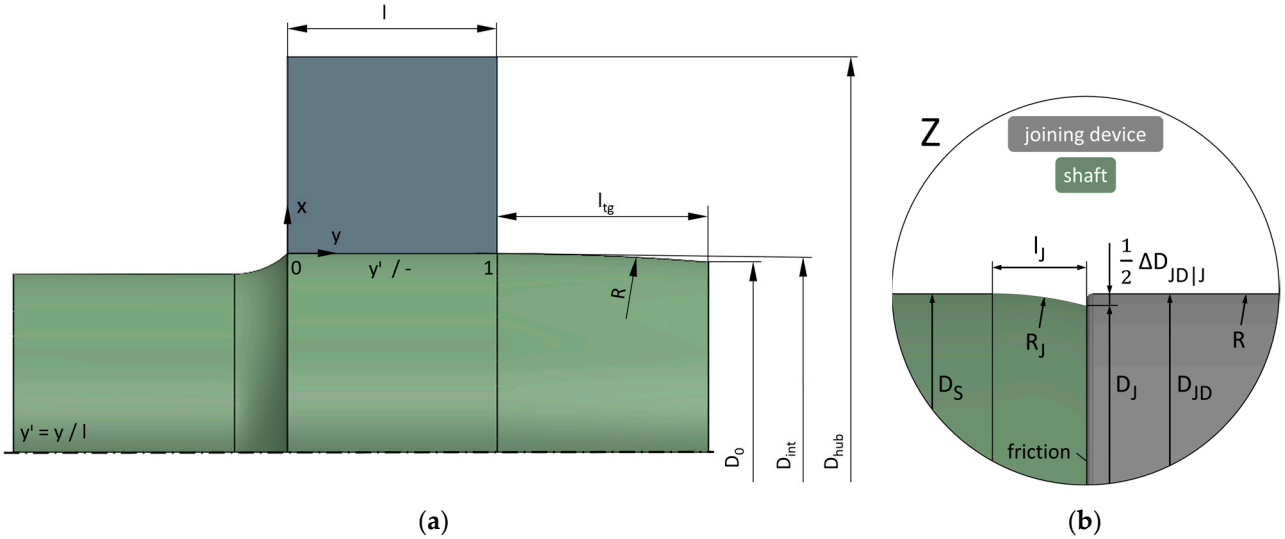

(**a**) (**b**)

Figure 2. (**a**) Geometry of the simulation model for transition radius analysis and (**b**) geometry of the simulation model for junction geometry analysis.

2. Definitions and Fundamentals

2.1. Definition of the Press–Fit Geometry

To analyze the influence of the joining device on the stress state of the press–fit connection, a comparability of the results with previous research, such as [7–13], must be ensured. The investigations in all of these publications focus on connections with a diameter of the interface of D_{int} = 30 mm, a diameter ratio of the hub of Q_{Hub} = 0.5, and a length–diameter ratio of about $l/D_{int} \approx 0.5$. The diameter ratio Q_{Hub} (cf., Equation (1)) is of particular interest, as it is, together with the selected material and interference ξ (cf., Equation (2)), a primary influence on the stress state, the hardening behavior, and consequently the transmission capacity of the investigated connection. The geometric interference I_{geo} is given in millimeters. It is necessary to calculate the interference ξ according to Equation (2). All remaining parameters needed to solve Equations (1) and (2) are defined in Table 1 and Figure 2 [8]:

$$Q_{Hub} = \frac{D_{int}}{D_{Hub}} \tag{1}$$

$$\xi = \frac{I_{geo}}{D_{int}} \cdot 1000\ [‰] \tag{2}$$

Table 1. Materials and geometry specification.

Material of the Shaft	Material of the Hub	Diameter Ratio of the Hub Q_{Hub}	Interference ξ Related to D_{int}	Diameter of the Interface D_{int}	Length-to-Diameter Ratio l/D_{int}
42CrMo4 +QT	EN AW-5083	0.5	10‰	30 mm	0.533

Therefore, the described geometry (cf., Figure 2a) was adopted, and the length–diameter ratio, in accordance with [8,9], was specified as l/D_{int} = 0.533. The material of the hub is aluminum wrought alloy EN AW-5083 (AlMg4.5Mn), and the material of the shaft is 42CrMo4 +QT, with a consistent interference of ξ = 10‰ applied throughout the analyses (cf., Table 1).

2.1.1. Geometry for Transition Radius Analyses

The geometry used to analyze the influence of the transition radius R on the stress state of the press–fit connection does not account for the junction geometry between the shaft and the joining device, since it is used specifically to evaluate the potential of large radii R. The length l_{tg} of the transition geometry is determined by the transition radius R used. The radius R ensures that the shaft becomes tapered towards its end face, resulting in a difference between the diameter of the shaft at its end face D_0 and the inner diameter of the hub D_{int} of 200 µm to account for tolerances and misalignments in the process (cf., Figure 2). The results are presented in Section 4.1. In the subsequent investigations, the modified transition radius R is applied to the joining device instead of to the shaft.

2.1.2. Geometry for Junction Geometry Analyses

As mentioned in Section 1, a second set of simulations is used to determine the influence of the junction between the shaft and the joining device on the stress state of the press–fit connection. Therefore, the junction geometry needs to be modeled explicitly. Hence, a radius R_J is applied to the shaft that accounts for misalignments and manufacturing tolerances of the shaft and the joining device to eliminate the risk of a front face collision between the shaft and the hub during the joining process. The interface between the shaft and the joining device is modelled using frictional contact (cf., Figure 2). The results of these investigations are presented in Sections 4.2 and 4.3.

3. Materials and Methods

3.1. Characterization of the Material Model

For the numerical investigations, the material properties of all materials used are required in order to be able to reliably calculate stress on the cylindrical press–fit connection. In accordance with Section 2.1 (cf., Table 1), tensile tests with precision strain measurements were carried out for the wrought aluminum alloy EN AW-5083 and the quenched and tempered steel 42CrMo4 +QT. The tensile specimens were taken from the same batch of material that was used for the experiments in Section 4.4. Table 2 shows the material properties which were ascertained with the experimental tensile tests.

Table 2. Material properties experimentally ascertained by uniaxial tensile tests.

Material	Young's Modulus E	Yield Strength $R_{p0.2}$	Tensile Strength R_m	Ultimate Strain A
42CrMo4 +QT	210 GPa	809 MPa	1081 MPa	14%
EN AW-5083	72 GPa	181 MPa	354 MPa	26%

In contrast to the elastic–ideal plastic design, the elastic–plastic design of cylindrical press–fit connections requires precise knowledge of the hardening behavior of the materials used. To describe the strain hardening behavior of the press–fit connection accurately, a non-linear material model is used. The model is based on the method of Li et al. [14], which allows for the combination of two parameterized Ramberg–Osgood [15] curves with a smooth transition [14,15]. This method was first adopted for press–fit connections by Kröger et al. [7,8] to account, with two different curves, for the varying hardening behavior occurring with increasing strain. Therefore, the Ramberg–Osgood model is extended by an index i (cf., Equation (3)) to approximate the region of low plastic strain with a curve corresponding to $i = 1$ and the region of large plastic strain with a curve corresponding to $i = 2$, respectively [8,14].

$$\varepsilon_{pl,i} = \left(\frac{\sigma_t}{K_i}\right)^{\frac{1}{m_i}} \text{ with : } i = 1{,}2 \mid \sigma_t : \text{ true stress} \mid K_i, m_i : \text{ model parameter} \tag{3}$$

According to Li et al. [14], the plastic strain ε_{pl} defined by the relationship between true plastic strain and true stress can be described as follows:

$$\varepsilon_{pl} = \frac{\varepsilon_{pl,2} \cdot e^{A \cdot \sigma_t + B} + \varepsilon_{pl,1}}{1 + e^{A \cdot \sigma_t + B}} \text{ with : } A,\ B : \text{ model parameter} \quad (4)$$

Between the experimental stress–strain curve and the material, model deviations were occurring for larger strains, which could be eliminated with a modification of the model by the approach of Hertelé et al. [7,8,16]. An iteratively determined amount $\Delta\varepsilon$ is used to shift the Ramberg–Osgood curve for the range of larger plastic strains in order to increase the accuracy of the model by changing Equation (3) to the following:

$$\varepsilon_{pl,2} - \Delta\varepsilon = \left(\frac{\sigma_t}{K_2}\right)^{\frac{1}{m_2}} \text{ with : } \sigma_t : \text{ true stress } | \ K_i, m_i : \text{ model parameter} \quad (5)$$

The high accuracy of the non-linear material model was validated using uniaxial tensile tests with precision strain measurements (cf., Figure 3) [7,8].

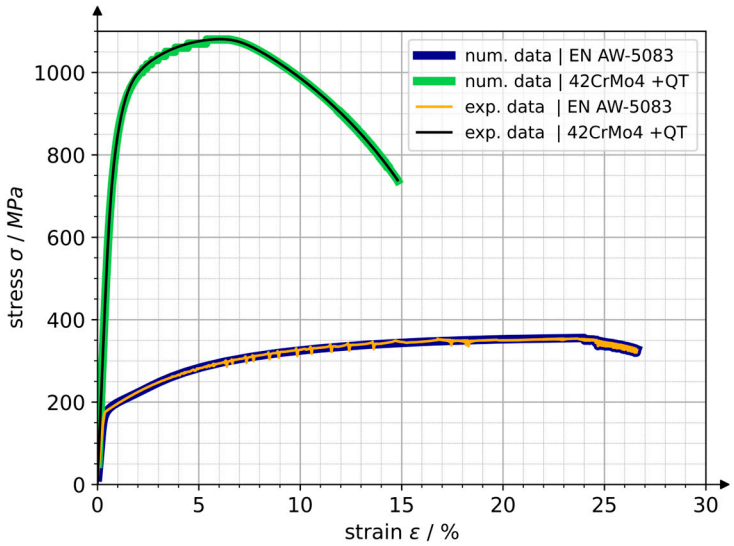

Figure 3. Validation of the material model (num. data) with experimental data (exp. data) based on [7,8].

The materials which were used for the shafts and hubs investigated in this research are from the same production lot as used in [7,8] to ensure comparability with these results. To rely on the numerical results of the finite element analysis, not only the material model but also the simulation model itself needs to be validated. An experimental procedure, described in Section 3.3, was used for this purpose [8].

3.2. Definition of the Finite Element Model Used for the Numerical Simulations

Finite element simulations are used to identify a suitable value for the transition radius R by analyzing the stresses and strains that occur and to ascertain the significance of the tolerances in the junction area between the shaft and the joining device. No further mathematical equations are required for this procedure, as the pressure distribution is approximated to the theoretical ideal (horizontal) distribution of the plane stress condition, according to [17]. Thus, no numerical optimization algorithms are needed. Due to the iterative approach, specific values for transition radii R and tolerances can be given as design recommendations, which are also useful for engineers in small- and medium-sized enterprises, where the financial and technical resources for complex numerical and mathematical optimizations are often limited.

The investigations described below were carried out using finite element analyses with ANSYS Workbench 2023 R1. Since the geometry investigated is axisymmetric, a 2D half model was used to simulate the joining process. Due to the significant deformations that the hub is subjected to as a result of the elastic–plastic design, the consideration of non-linearities and large deformations are activated in the software. The sample geometry—consisting of a shaft, a joining device, and a hub—is completed by a support for the hub, which is used to absorb the joining forces (cf., Figure 1). The support is rigidly fixed on its rear surface, whereas the contacts between the individual components are subjected to friction. The coefficient of friction in the contact area between the hub and the shaft, respectively, with the joining device, was set to μ = 0.08, based on empirical values from [7]. The remaining contacts were set to a coefficient of friction of μ = 0.1—in accordance with [17]. As a contact algorithm, the augmented Lagrange method was chosen, which proved to be suitable here, in conformity with [7]. The contact penetration tolerance was set to a maximum of 1 µm, as excessive penetration could change the interference ξ and thus the occurring stresses. Finally, the finite element model was meshed, whereby the element size was determined by means of a convergence study (cf., Figure 4).

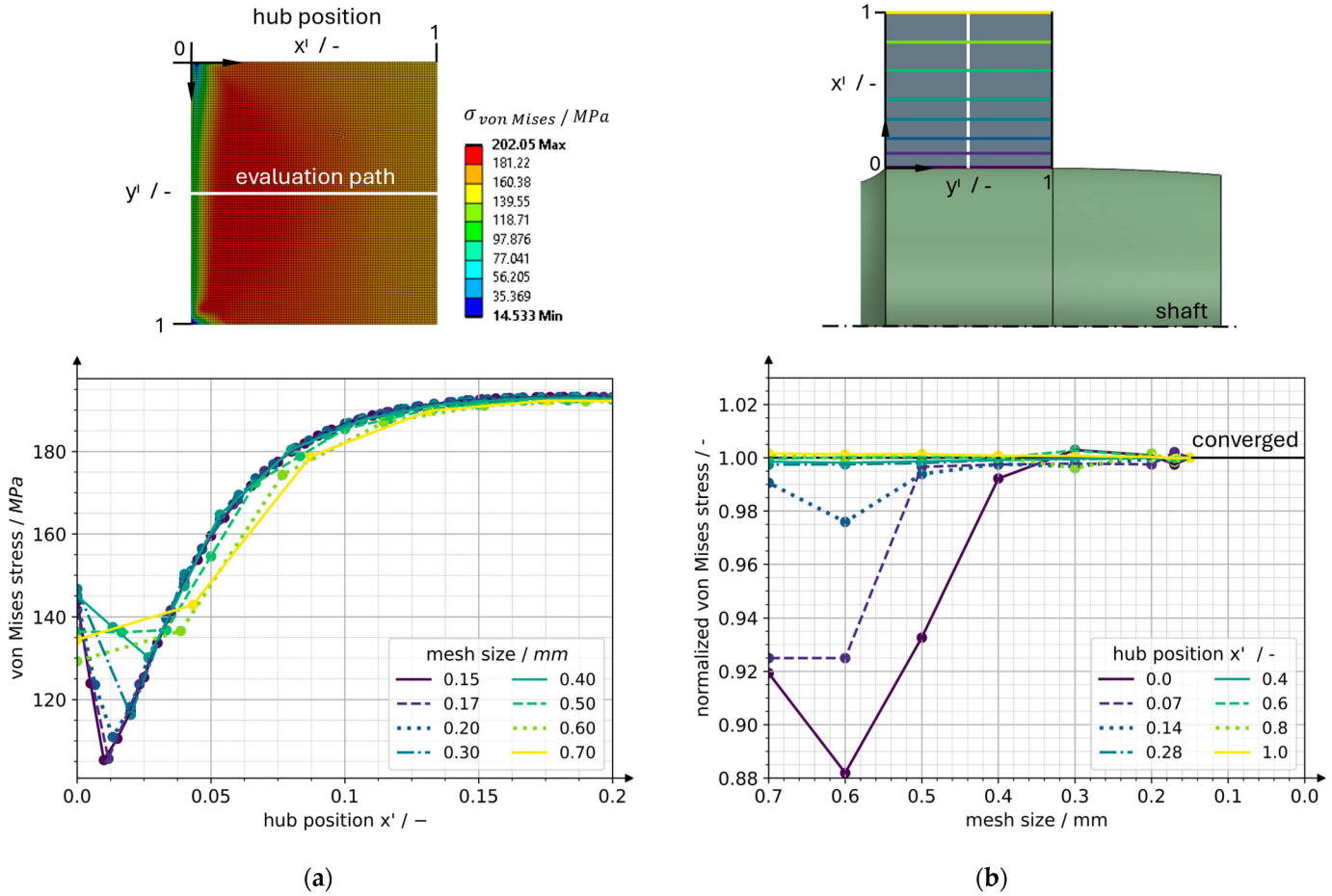

(**a**) (**b**)

Figure 4. Mesh-convergence study to determine the mesh size. (**a**) von Mises stress for different mesh sizes along the evaluation path. (**b**) Convergence behavior depending on the mesh size at different positions in the hub.

The convergence study demonstrates that in the outer area of the hub, where the stresses are lower, the calculation already converges with element sizes of 0.7 mm (cf., Figure 4). In contrast, significantly smaller elements are required in areas close to the contact between the shaft and hub (cf., Figure 4) to achieve convergence. In the radial direction x′, the hub was divided into two areas with different mesh sizes based on the convergence study in Figure 4. The area x′ $\leq$ 0.267 was meshed with an element size of

0.15 mm. In the area closer to the outside of the hub ($0.267 < x' \leq 1.0$), the element size was set to 0.7 mm. The calculation results were visualized either in ANSYS Workbench (graphical illustrations) or using Python on the basis of the exported raw data (diagrams).

3.3. Experimental Procedure for the Validation of the Simulation Model

The experimental validation of the simulation model was performed in accordance with previous research [7,8,18,19]. The method utilizes the proportionality between the geometric changes of the hub related to deformation and the pressure within the interface p. For this, the approach is comparing numerically and experimentally determined deformations of the hub. With an experimental procedure containing measuring the components before and after joining, the change in diameter of the hub can be calculated and compared to the numerically determined data. Due to the proportionality between the deformation of the hub and the pressure within the interface p as described above, the simulation results can be validated by experimentally determining the hub deformation on a coordinate measuring machine. Unfortunately, there is currently no method for measuring the pressure directly in the contact surface. With the experimental procedure shown in Figure 5, the simulation model that was used in Section 4 of this research article was validated [8].

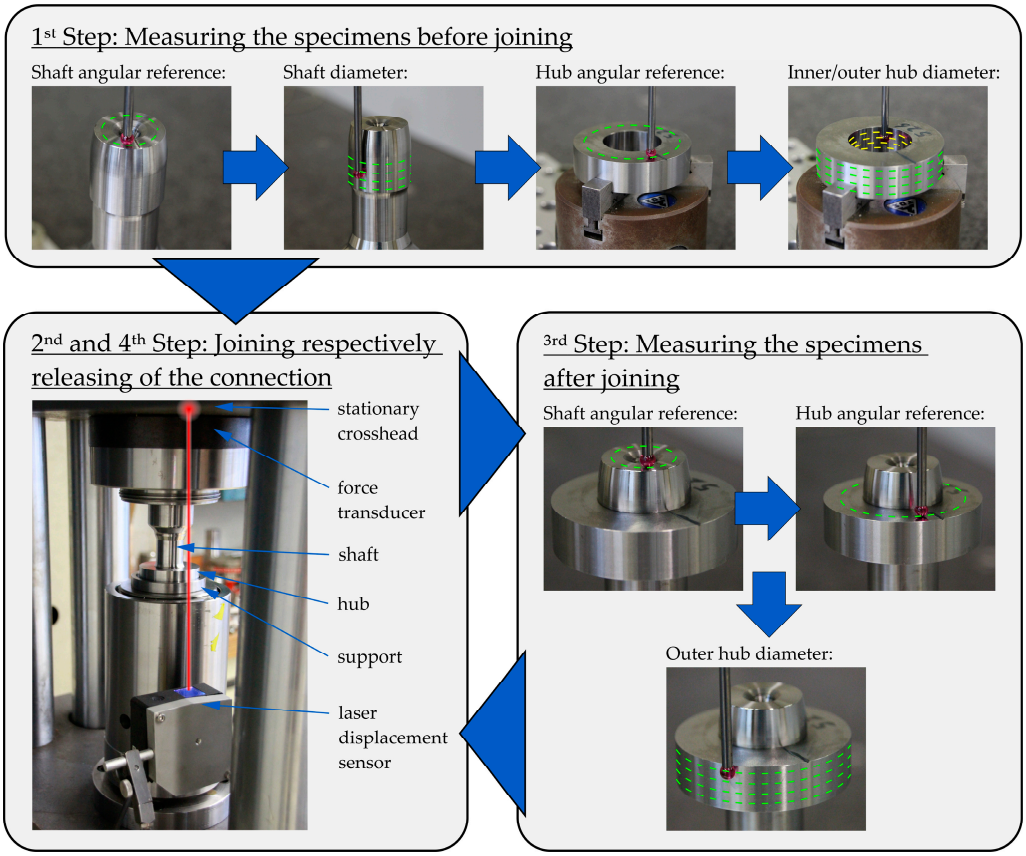

Figure 5. Experimental procedure validating the numerical results according to [8].

4. Results

4.1. Analysis of the Effect of Large Transition Radii R on the Stress State of the Press–Fit Connection

The numerical simulation of the joining process, as described in Section 2.1.1, shows that augmenting the transition radius R (cf., Figure 2) increases the average pressure between shaft and hub by reducing the pressure loss in the axial center region of the hub (cf., Figure 6). Moreover, pressure maxima are reduced, leading to increased fatigue strength. This is particularly beneficial for press–fit connections that are subject to bending moments that introduce further radial stresses, eventually approaching a stress state critical

to failure. Both the increase in average pressure and the reduction in pressure peaks correlate with the homogenized plastic strain distribution along the connection length that is achieved through larger transition radii R. For small radii R, this distribution is characterized by a localized peak at the inner edge of the hub ($y' = 0$) and by an increase in strain at the center of the hub ($y' = 0.5$) as depicted by the green semi-parabolic area (cf., Figure 6). The latter phenomenon is caused by joining forces, which similarly increase when the center part of the hub crosses the transition radius R.

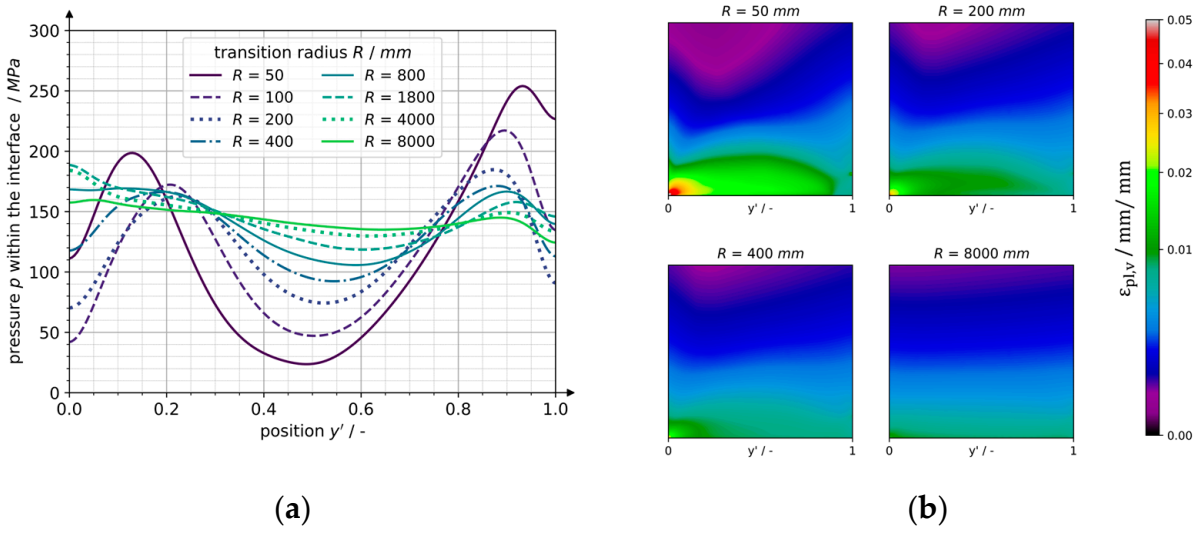

Figure 6. (**a**) Pressure distribution and (**b**) equivalent strain distribution in the hub. Both have a variation of the transition radii R for interference of $\xi = 10‰$, shaft made from 42CrMo4 +QT, and a hub made from EN AW-5083.

The stress state of the hub resulting in the joining process is dependent on the geometry of the press–fit connection (D_{int}, Q_{Hub}, l, and R) and on the interference ξ in particular. The quantitative evaluation of the aforementioned joining process shows that a transition radius of $R = 8000$ mm achieves an almost constant pressure (cf., Figure 6) as well as a homogenized plastic strain distribution. This value presents a limit to the significant improvement of the stress state of the press–fit connection, after which further increasing of the transition radius R is, in particular with respect to the anticipated manufacturing tolerances and lubrication challenges, not beneficial. From a pressure distribution for the interference of $\xi = 10‰$, it can be determined that a radius variation in the lower range $R < 500$ mm has a significant impact, corresponding to a reduction in pressure losses in the center of the hub of 58% for a radius increase from $R = 50$ mm to $R = 400$ mm. Increasing the radius R further leads to additional contributions to the homogeneity of the pressure p and plastic strain distribution, reaching a maximum reduction in pressure loss of 92% and a 22% increase in mean pressure in the connection for a transition radius of $R = 8000$ mm compared to the reference geometry with $R = 50$ mm.

4.2. Analysis of the Junction Geometry on Its Influence on the Stress State of the Press–Fit Connection

Resulting from the concept of a detachable joining device, the hub must overcome the junction between the joining device and shaft (cf., Figures 1 and 2). It must be considered that manufacturing tolerances do not allow for a sharp-edged junction as ideally assumed in Section 4.1. Due to inevitable manufacturing deviations, it is essential to apply a junction geometry that mitigates diametral differences and certain tolerances between the joining device and the shaft. Thus, a junction radius R_J on the shaft is introduced, which leads to a junction diameter D_J that is smaller than the diameter of the joining device D_{JD}, creating a difference between the diameters $\Delta D_{JD\,|\,J}$ (cf., Figure 2). This diametral difference $\Delta D_{JD\,|\,J}$

prevents the critical case of frontal contact between the shaft and the hub by allowing for manufacturing tolerances and misalignments proportional to its size.

To determine the influence of this radius R_J on the stress state of the press–fit connection, a simulation series is performed in which the junction radius R_J is systematically varied. Considering that a large radius R_J would diminish the advantages of a joining device in terms of its purpose to reduce the overall size of the shaft–hub connection, the unused length l_J of the shaft resulting from the radius R_J is restricted to a maximum of 1.5 mm. This is even less then the length of the transition geometry of a common press–fit connection, according to the design guideline of the German standard DIN 7190-1 [17].

The analysis shows that increasing the diametral difference $\Delta D_{JD\,|\,J}$, while leading to an improved assembling process safety, simultaneously decreases the transmission capacity by reducing the pressure p in the connection, establishing a corresponding trade-off (cf. Figure 7). However, the use of a joining device with a junction geometry with $\Delta D_{JD\,|\,J}$ = 200 µm that allows for significant manufacturing tolerances and misalignments without an impairment of the joining process still achieves 90% of the average pressure that was obtained for a transition radius of R = 8000 mm in Section 4.1 while decreasing the unused length of the shaft from l_{tg} = 63 mm to $l_{tg} = l_J$ = 1.5 mm by 98%. The analysis of the sensitivity of the pressure distribution to the size of the diametral difference $\Delta D_{JD\,|\,J}$ for a press–fit connection with an interference of ξ = 10‰ shows that decreasing $\Delta D_{JD\,|\,J}$ from 200 µm to 50 µm would allow for an increase in pressure of 6%.

Based on the analysis of the influence of large transition radii R and of the junction geometry on the stress state of the press–fit connection, the potential of the joining device in lightweight applications can be evaluated. The achieved reduction in pressure loss, the increase in average pressure, and therefore the increased transmission capacity are functions of the transition radius R employed (cf., Section 5). This transition radius in the current elastic–plastic design of press–fit connections without a joining device leads to a large non-usable shaft length l_J (cf., Section 5) that increases the mass and the size of the drive system substantially. The detachable joining device enables the implementation of large transition radii R, while maintaining a small non-usable shaft length of l_J = 1.5 mm on the shaft itself with only a small reduction in the force and torque transmission capacity compared to the idealized geometry shown in Section 4.1. The joining device therefore has the potential to significantly decrease the mass and installation space, yielding a substantial benefit in force and torque transmission as well as in lightweight applications (cf., Figure 8; cf., Table 3). With the presented joining device, the shaft geometry (a) can be used, which leads to a reduction in mass and length of 70% or 95% (compared to the shaft geometry (b), respectively, (c), as shown in Figure 8 and Table 3).

Table 3. Length and mass of different transition geometries and corresponding reductions achieved by using a joining device.

	Shaft Geometry	Length of the Radius Geometry	Mass of the Radius Geometry
(a)	using a joining device to achieve an improved pressure distribution with R = 8000 mm and $\Delta D_{JD\,|\,J}$ = 200 µm (cf., Figure 7a)	l_1 = 1.5 mm	8.3 g
(b)	used to achieve the reference pressure distribution with R = 50 mm (cf., Figure 7a)	l_2 = 5.0 mm	27.4 g
(c)	necessary to achieve the same pressure distribution as shaft geometry (a) without using a joining device	l_3 = 28 mm	153.8 g

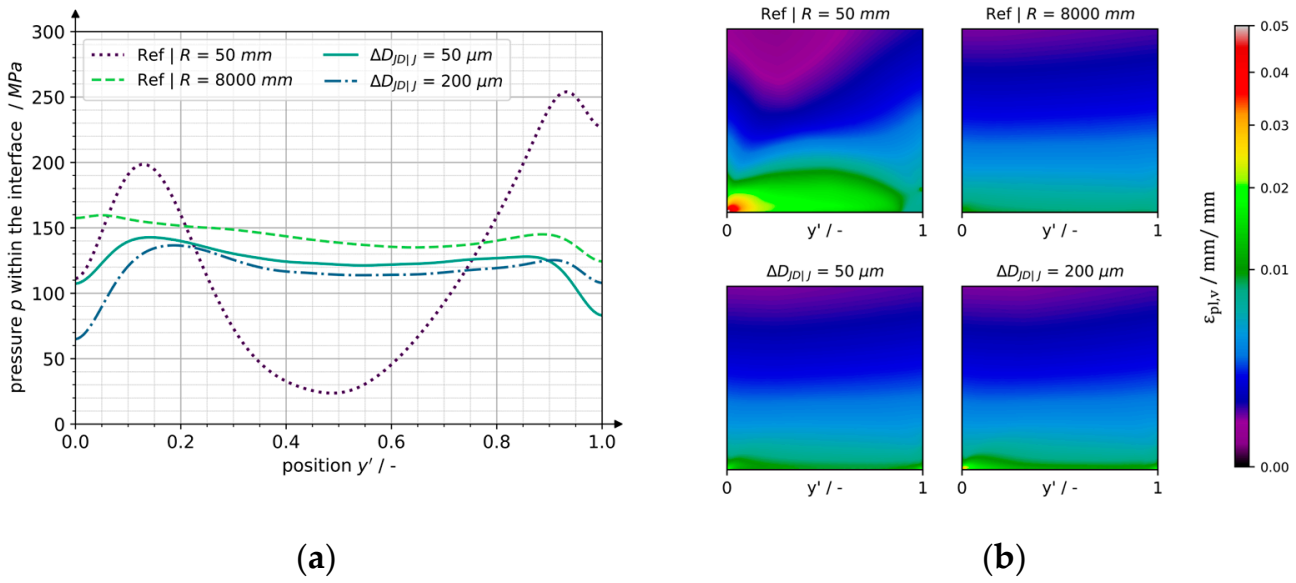

Figure 7. (**a**) Pressure distribution and (**b**) equivalent strain distribution in the hub. Both with a variation in the junction geometry for interference of ξ = 10‰, a shaft made from 42CrMo4 +QT, and a hub made from EN AW-5083.

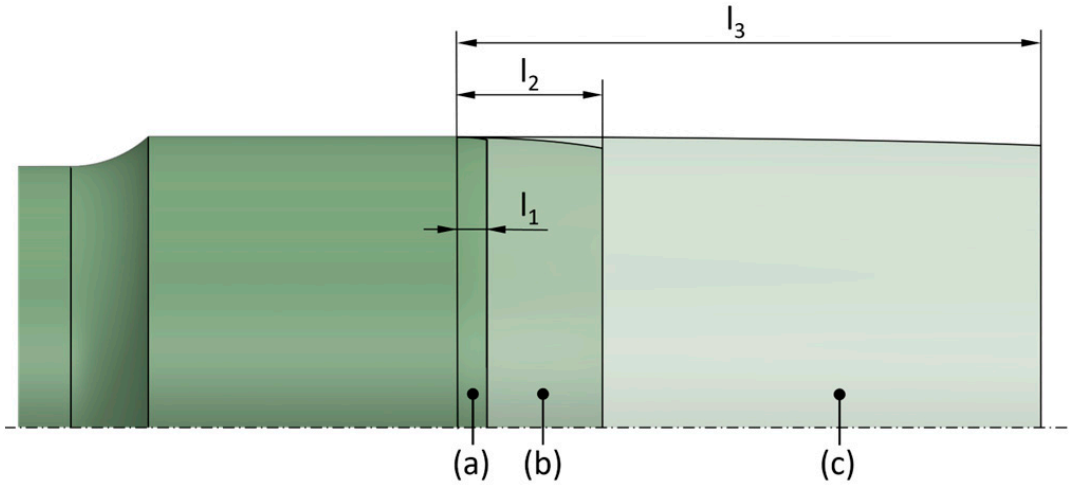

Figure 8. Shaft geometry: (**a**) small transition radius when using a joining device, (**b**) reference geometry with a transition radius of R = 50 mm (not to scale), and (**c**) large transition radius to achieve the same result as (**a**) without a joining device.

4.3. Analysis of Manufacturing Tolerances on Their Influence on the Stress State of the Press–Fit Connection

The proposed junction geometry ensures a secure joining process by accommodating anticipated manufacturing tolerances. However, the diameters of the shaft D_S and the joining device D_{JD} are still affected by tolerances, meaning that two further cases can arise in contrast to the assumption $D_S = D_{JD}$ made in Section 4.2. The following analysis targets the diametral difference between the joining device and the shaft $\Delta D_{JD\,|\,S}$, considering the two cases that either the diameter of the shaft D_S is larger than the diameter of the joining device D_{JD} (cf., Section 4.3.1 and Figure 9) or vice versa (cf., Section 4.3.2 and Figure 10). The results should assess the impact of these tolerances on the transmission capacity of the press–fit connection and the extent to which the potential of the joining device is diminished as a result.

4.3.1. Case of a Larger Shaft Diameter D_S

Joining a press–fit connection using a joining device with a diameter D_{JD} that is smaller than the diameter of the shaft D_S leads to partly opposing phenomena depending on the size of the diametral difference $\Delta D_{JD|S}$. Up to a certain limit (here, $\Delta D_{JD|S}$ = 40 µm), an increasing diameter of the shaft D_S caused by manufacturing tolerances induces additional interference ξ that increases the transmission capacity by slightly raising the pressure near to the axial center ($y' \approx 0.35$) of the shaft–hub connection. Once the difference between the joining device and shaft diameter $\Delta D_{JD|S}$ becomes too large (here, $\Delta D_{JD|S}$ = 80 µm), the prevailing phenomenon is a pressure loss that occurs at $0.2 \leq y' \leq 0.7$ (cf., Figure 9), which is caused by the increasing joining force required to overcome the additional interference ξ at the small radius of the joining geometry R_J (cf., Figure 2), similar to the more severe pressure loss caused by a small transition radius R that is described in Sections 1 and 4.1. Numerical investigations show that the latter phenomenon becomes predominant as soon as the tolerance exceeds $\Delta D_{JD|S}$ = 40 µm with stress extrema and local plastic deformations significantly increasing after surpassing this threshold. Basically, since the diameter of the shaft is larger than that of the joining device, high plastic deformations occur in the area of the inner hub edge when it comes in contact with the shaft radius R_J during the joining process. These plastic deformations did not occur for the reference geometry (cf., Section 4.2), since the diameters of the shaft and the joining device are the same and therefore no additional interference ξ has to be overcome at the small radius R_J of the shaft.

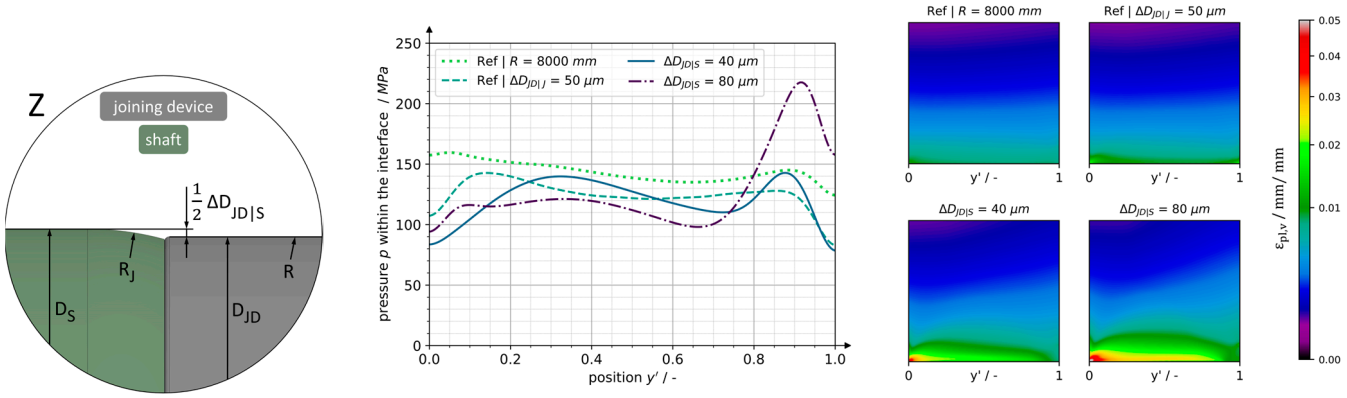

Figure 9. (**a**) Simulation geometry for varying tolerances between the shaft (larger) and joining device, (**b**) pressure distribution, and (**c**) equivalent plastic strain in the hub. For both, (**b**,**c**), tolerance between the shaft (larger) and joining device is varied for an interference of ξ = 10‰, the shaft is made from 42CrMo4 +QT, and the hub is made from EN AW-5083.

4.3.2. Case of a Larger Joining Device Diameter D_{JD}

A numerical analysis of manufacturing tolerances that lead to a diameter of the shaft D_S that is smaller than the diameter of the joining device D_{JD} (cf., Figure 10) shows that this case decreases the transmission capacity of the press–fit connection significantly. This is caused by the plastic deformation occurring at the inner diameter of the hub due to the large interference ξ that restricts the elastic recovery of the hub to a smaller diameter. The analysis shows that the pressure p decreases proportionately to the tolerance $\Delta D_{JD|S}$, with a pressure loss of approximately Δp = 12.5 MPa for each $\Delta D_{JD|S}$ = 10 µm increase in tolerance (cf., Figure 10).

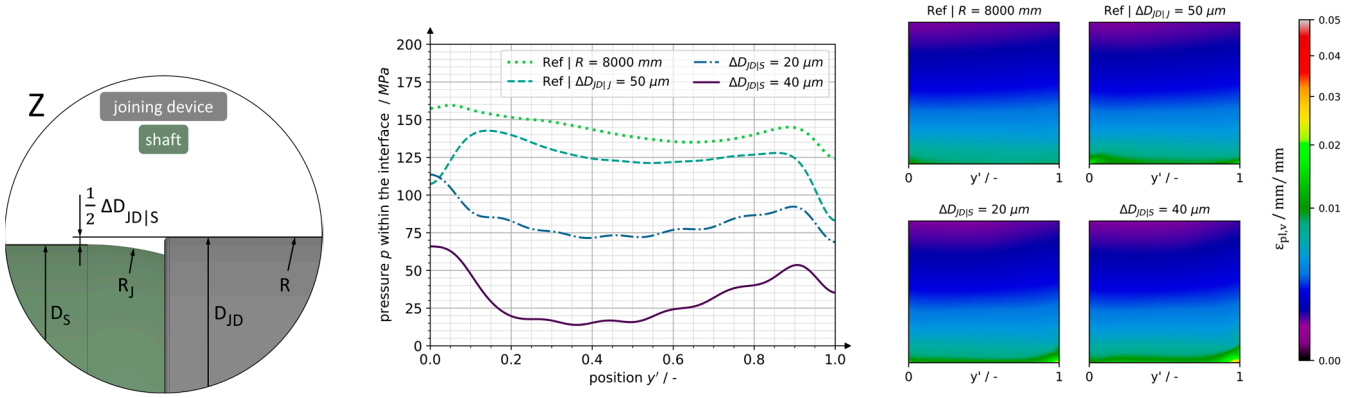

(**a**) (**b**) (**c**)

Figure 10. (**a**) Simulation geometry for varying tolerances between the shaft (smaller) and joining device, (**b**) pressure distribution, and (**c**) equivalent plastic strain in the hub. For both, (**b**,**c**), tolerance between the shaft (smaller) and joining device is varied for an interference of ξ = 10‰, the shaft is made from 42CrMo4 +QT, and the hub is made from EN AW-5083.

The localized plastic deformations occur not as previously observed at the front edge of the hub but rather at the rear edge, as the load-bearing area gradually focuses on the rear part of the hub when crossing the junction geometry (cf., Figure 10). Concluding from this analysis, the upper deviation limit of the diameter of the joining device should not exceed the lower deviation limit of the shaft diameter.

4.4. Experimental Validation

To validate the numerical results, the geometry of the shaft and the associated joining device were designed based on the findings from Section 4.1 to Section 4.3. The transition radius of the joining device was selected as R = 4000 mm (Section 4.1), the diameter difference as $\Delta D_{JD|J}$ = 200 µm, and the diameter difference as $\Delta D_{JD|S}$ = 20 µm (Section 4.3). The specimens were then manufactured in the institute's workshop from the materials intended for this purpose (cf., Figure 11), considering the other geometry parameters (cf., Table 1). The joining device is centered in the shaft by a short pin to ensure radial alignment. Due to a suitable tolerance (Ø8 H7/g6), this pin ensures that, for the coaxiality of both the shaft and joining device, no collision can occur between their end faces, thus guaranteeing a reliable joining process.

(**a**) (**b**)

Figure 11. (**a**) Specimens before joining and (**b**) press–fit connection after the joining process.

The procedure presented in Section 3.3 for validating the numerical calculation results, which is based on a comparison of the hub expansion, was carried out with the defined geometry. The joining experiment was carried out on a hydraulic press, which can achieve a maximum joining force of 250 kN. This ensures the required force avoids stick slip, which is recommended according to [17].

The axial force during the experiment was recorded using a force transducer. A laser sensor was used to record the joining distance of the press–fit connection, which corresponds to the change in the distance measured between the laser sensor and the stationary crosshead of the hydraulic press (cf., Figure 5). The accuracy of the measurement is 2000 data points within one second. Figure 12 shows the force during joining. Due to the very large transition radius of R = 4000 mm of the joining device, the interference ξ is overcome across a long distance. This leads to low and very evenly increasing joining forces (cf., s < 32 mm in Figure 12), which is also beneficial for the stress distribution in the hub and leads to a uniform pressure in the interface of the connection (cf., Figure 6 and [8]). Starting from s > 32 mm, the hub is forced onto the cylindrical shaft, whereby only a slight interference ξ at the radius R_J has to be overcome. However, this happens along a significantly shorter axial distance of l_J = 1.5 mm, causing the gradient of the force curve in Figure 12 to increase. After the joining process, the joining device can be removed manually from the shaft and reused for the next press–fit connection (cf., Figure 11). For mass production, the joining device can be finished with a DLC coating (diamond-like carbon), for example, to increase the durability of the device.

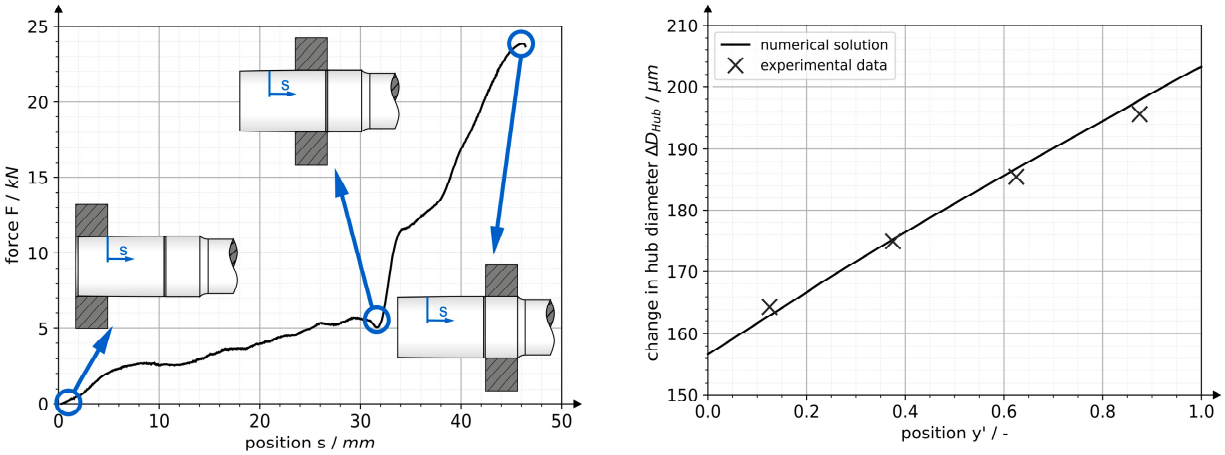

Figure 12. (**a**) Force during joining the press–fit connection using a joining device and (**b**) changes in hub diameter used for validation purposes.

The validation of the numerical results is completed by comparing the change in hub diameter between the experiment and the simulation. For this purpose, the specimens were measured on a coordinate measuring machine before and after the joining process, as described in Section 3.3. This first enabled a simulation of the joining process with the actual dimensions of the specimen and second, the determination of the hub expansion in the experiment. The latter was compared with the numerically calculated hub expansion in Figure 12. This clearly shows that the absolute values of the simulation and experiment deviate from each other by less than 3 µm (less than 2%). The numerically determined results from Section 4 can therefore be considered valid.

5. Discussion

5.1. Discussion and Design Recommendation

Consolidating the outcomes from Section 4 provides a foundation of information on which a design recommendation can be formulated. Section 4.1 demonstrates the

potential of large transition radii R for homogenizing the pressure distribution and therefore increasing the transmission capacity of press–fit connections. Sections 4.2 and 4.3 analyze the influence of the detachable joining device that enables this transition geometry for practical applications.

The results obtained in Section 4.1 suggest that increasing the transition radius R of the shaft from the reference radius from R = 50 mm to R = 8000 mm reduces the pressure loss that occurs for large interferences ξ in the center of the hub by 90% (cf., Figure 6). Assuming a difference between the diameter of the shaft at the connection to the hub D_0 and the inner diameter of the hub D_{int} of 200 µm to account for tolerances and misalignments in the process, this results in a non-usable shaft length of the transition geometry of $l_{tg} \approx 63$ mm (cf., Figure 2). This is not achievable in most applications due to restrictions on the mass and installation space.

The numerical analysis of the detachable joining device used to substitute this transition geometry (cf., Section 4.2) shows that despite the required junction geometry (cf., Figure 1), an average pressure of 90% of the pressure distribution, which was achieved for the transition geometry without a junction and with a radius of R = 8000 mm (cf., Section 4.1), can be realized (cf., Figure 13). Moreover, 78% of the pressure loss in the hub center seen for the reference radius of R = 50 mm can be recovered. Using this joining device therefore leads to a significant increased transmission capacity with a shaft radius R_J with an axial length l_J limited to 1.5 mm (cf., Figure 7), which is 92% less than the non-usable length l_{tg} (cf., Figure 2) necessary to achieve the same result without a joining device (cf., Figure 13).

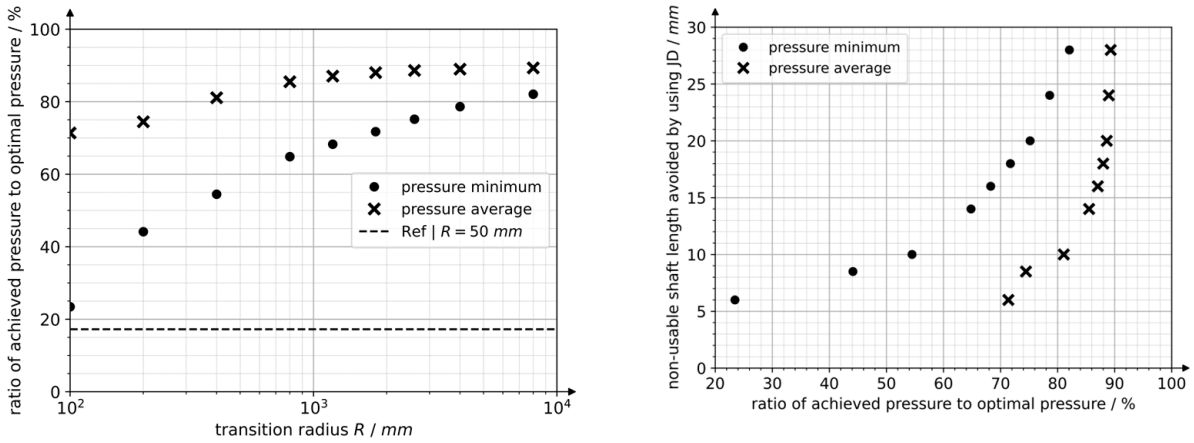

Figure 13. (**a**) Achieved pressure ratio for varying transition radii R and (**b**) non-usable shaft length avoided by using a joining device and the achieved pressure ratios.

Furthermore, the results of Section 4.2 present a relation between the pressure distribution and the diametral difference $\Delta D_{JD|J}$ (cf., Figure 7) that defines the maximal tolerances of the parts that can be accommodated and is therefore a measure for process safety. Increasing this diametral difference from $\Delta D_{JD|J}$ = 50 µm, which was used to achieve the aforementioned 78% pressure loss reduction, to $\Delta D_{JD|J}$ = 200 µm, which allows for significant manufacturing tolerances, only results in a 7% pressure decrease. This demonstrates the sensitivity of the pressure distribution and therefore the transmission capacity of the press–fit connection to the junction geometry needed to accommodate manufacturing tolerances. However, it does not present information on the influences of tolerances themselves that are analyzed in Section 4.3.

Focusing on the diametral difference between the joining device and the shaft $\Delta D_{JD|S}$, this tolerance leads to two different cases where either the diameter of the shaft D_S is larger than the diameter of the joining device D_{JD} or vice versa. The results show that

the upper deviation limit of the shaft diameter should not exceed the lower deviation limit of the joining device diameter by more than 40 µm (cf., Section 4.3.1) to prevent pressure maxima that can be critical in cyclic loading conditions for connections that are subject to bending stresses, especially for materials with limited ductility. Furthermore, the upper deviation limit of the joining device should never exceed the diameter resulting from the lower deviation limit of the shaft. Such tolerances show a rapid reduction in the transmission capacity, corresponding to a 10% pressure drop in the center of the hub per 10 µm tolerance, causing the diameter of the joining device to exceed the diameter of the shaft (cf., Section 4.3.2). Consolidating these findings into a recommendation for allowable manufacturing tolerances results in the tolerance field presented in Figure 14. Considering other geometries and materials, a general application of this recommendation has been identified. With these findings, the tolerance recommendation is 1.33‰ of D_{int}.

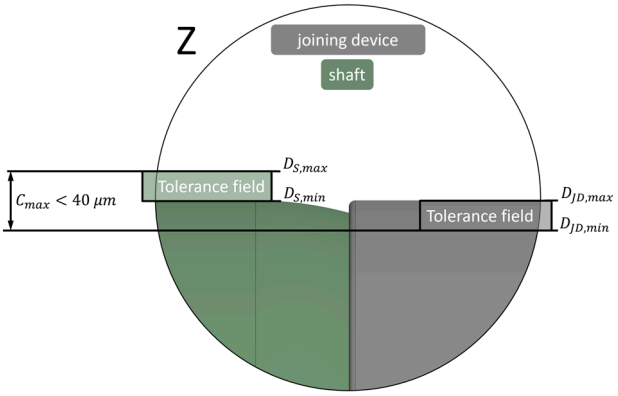

Figure 14. Proposed tolerances of junction geometry to maximize transmission capacity.

5.2. Summary of Key Findings

The key findings obtained from the presented research results are summarized in Table 4.

Table 4. Key findings obtained from discussed research results.

	Finding	Details and Recommendations	Section
(1)	Large transition radii R for increased transmission capacity	The pressure reduction Δp occurring for the elastic–plastic press–fit connection in the axial hub center can be reduced by 85% for a transition radius of R = 4000 mm and up to 90% for R = 8000 mm compared to the reference radius of R = 50 mm.	Section 4.1
(2)	Detachable joining device as enabler for large transition radii R in practical applications	The axial length of large transition radii R described in row (1) prevents their use in most applications, if these are conventionally provided as part of the shaft. Using a detachable joining device enables the use of such large transition radii R to obtain up to 90% of the pressure achieved in row (1) with a 95% reduction in the non-usable shaft length.	Sections 4.2 and 5.1
(3)	Design recommendation for reduced susceptibility to manufacturing tolerances	Identified tolerance fields for an improved transmission capacity (cf., Figure 14): • The upper deviation limit of the shaft should not exceed the lower deviation limit of the joining device by more than 40 µm. • The upper deviation limit of the joining device should never exceed the lower deviation limit of the shaft.	Sections 4.3 and 5.1

6. Conclusions

The results of this research article suggest the capability of a detachable joining device to enable the threefold increase in transmission capacity achieved by employing elastic–plastic instead of elastic press–fit connections. Large transition radii of the shaft that are necessary to join these connections often prevent this shaft–hub connection from being used in practical applications because of limitations in the mass and installation space. Substituting this transition geometry with a detachable joining device results in a significant reduction in the mass and installation space of the connection.

This article presents design recommendations on joining devices for elastic–plastic press–fit connections. For the first time, the possibility of separating the transition radius, which is generally necessary for press–fit connections to overcome geometric interferences, from the shaft by means of a detachable joining device is investigated. This results in the following advantages:

(1) The axial length of the transition radius and thus its size are no longer restricted by the installation-space limits of the assembly.
(2) The mass of the press–fit connection will not be affected by the size of the transition radius.

Using experimentally validated finite element simulations, this research article presents, in detail, the impact of large transition radii and manufacturing tolerances of a detachable joining device on stresses, strains, and force and torque transmissions in a press–fit connection. Finally, generalized design recommendations are given for the user, which can also be applied to other geometries and materials. The novel recommendations are as follows:

(1) A transition radius of at least 4000 mm should be selected for a high mean value of the pressure between the shaft and hub, as well as a uniform distribution of the pressure and the plastic strains.
(2) The upper limit of the joining device's tolerance field should never exceed the lower limit of the shaft's tolerance field.
(3) The upper limit of the shaft's tolerance field should not exceed the lower limit of the joining device's tolerance field by more than 1.33‰ of the diameter of the contact interface.

Therefore, the results significantly contribute to extending the application of elastic–plastic-designed press–fit connections. As a result, the performance of technical systems can be increased and the use of resources in production and operations can be reduced, thus achieving an important impact on resource protection.

Author Contributions: Conceptualization, J.F. and D.H.; methodology, J.F and D.H.; software, J.F. and D.H.; validation, J.F.; formal analysis, J.F.; investigation, J.F. and D.H.; resources, J.F.; data curation, J.F.; writing—original draft preparation, J.F. and D.H.; writing—review and editing, J.F.; visualization, J.F. and D.H.; supervision, H.B. and M.K.; project administration, H.B. and M.K.; funding acquisition, H.B. All authors have read and agreed to the published version of the manuscript.

Funding: The research presented here is based on results of experiments that were funded by the Federal Ministry for Economic Affairs and Climate Action on the basis of a decision by the German Bundestag (IGF project no.: 19621 N).

Institutional Review Board Statement: Not applicable.

Informed Consent Statement: Not applicable.

Data Availability Statement: The data presented in this study are available on request from the corresponding author.

Conflicts of Interest: The authors declare no conflicts of interest.

References

1. Dausch, V.; Kröger, J.; Kreimeyer, M. An AI-Based Approach to Optimize Stress in Shrink Fits. *Proc. Des. Soc.* **2022**, *2*, 1549–1558. [CrossRef]
2. Gamer, U. The Rotating Elastic-Plastic Shrink Fit with Hardening. *Acta Mech.* **1986**, *61*, 15–27. [CrossRef]
3. Gamer, U. The Shrink Fit with Elastic-Plastic Hub Exhibiting Constant Yield Stress Followed by Hardening. *Int. J. Solids Struct.* **1987**, *23*, 1219–1224. [CrossRef]
4. Kittsteiner, J.; Ehrlenspiel, K. *Kostenanalyse von Welle-Nabe-Verbindungen in Zahnradgetrieben—Abschlussbericht zum FVA-Forschungsvorhaben Nr. 134, Heft 293*; Forschungsvereinigung Antriebstechnik e.V.: Frankfurt, Germany, 1989.
5. Kollmann, F.G. *Welle-Nabe-Verbindungen—Gestaltung, Auslegung, Auswahl*; Springer: Berlin/Heidelberg, Germany, 1984. [CrossRef]
6. Baldanzini, N. A General Formulation for Designing Interference-Fit Joints with Elastic-Plastic Components. *J. Mech. Des.* **2004**, *126*, 737–743. [CrossRef]
7. Kröger, J.; Binz, H. *Untersuchungen zu Auslegungsgrenzen und Steigerung der Maximalen Übermaße bei Zylindrischen Pressverbindungen—Abschlussbericht zum FVA-Forschungsvorhaben Nr. 810 I, Heft 1399*; Forschungsvereinigung Antriebstechnik e.V.: Frankfurt, Germany, 2020.
8. Falter, J.; Binz, H.; Kreimeyer, M. Investigations on design limits and improved material utilization of press-fit connections using elastic-plastic design. *Appl. Eng. Sci.* **2023**, *13*, 1–14. [CrossRef]
9. Önöz, I.E. *Die Auslegung Elastisch-Plastisch Beanspruchter Querpressverbände Unter Berücksichtigung der Werkstoffverfestigung*; VDI-Verlag: Düsseldorf, Germany, 1983.
10. Glöggler, C. Untersuchungen an Spannungshomogenisierten und Zylindrischen Pressverbindungen unter Torsionsbelastung. Dissertation, Universität Stuttgart, Stuttgart, Germany, 2003.
11. Blacha, M. Grundlagen zur Berechnung und Gestaltung von Querpressverbänden mit Naben aus Monolithischer Keramik. Dissertation, Universität Stuttgart, Stuttgart, Germany, 2009.
12. Heydt, J.F. Untersuchungen zum Dynamischen Verhalten von Topologisch Optimierten Pressverbänden bei Umlaufbiegung. Dissertation, Universität Stuttgart, Stuttgart, Germany, 2012.
13. Lohrengel, A.; Schäfer, G.; Mänz, T. *Untersuchung von Pressverbindungen mit gerändelter Welle—Abschlussbericht zum FVA-Forschungsvorhaben Nr. 658 I, Heft 1247*; Forschungsvereinigung Antriebstechnik e.V.: Frankfurt, Germany, 2017.
14. Li, T.; Zheng, J.; Chen, Z. Description of full-range strain hardening behavior of steels. *SpringerPlus Eng.* **2016**, *5*, 1316. [CrossRef]
15. Ramberg, W.; Osgood, W.R. *Description of Stress-Strain-Curves by Three Parameters*; NACA Technical Note No. 902; National Advisory Committee for Aeronautics (NACA): Washington, DC, USA, 1943.
16. Hertelé, S.; De Waele, W.; Denys, R. A generic stress-strain model for metallic materials with two-stage strain hardening behavior. *Int. J. Non-Linear Mech.* **2011**, *46*, 519–531. [CrossRef]
17. *DIN 7190-1:2017-02*; Interference Fits—Part 1: Calculation and Design Rules for Cylindrical Self-Locking Pressfits. Beuth: Berlin, Germany, 2017.
18. Ulrich, D.; Binz, H. Einfluss von Schmierstoffen aus der Massivumformtechnik auf die Reibdauerbeanspruchung mikroschlupfanfälliger Welle-Nabe-Verbindungen—Numerische und experimentelle Untersuchungen anhand zylindrischer Querpressverbände mit beschichteten Wellen unter wechselnder Torsionslast. In Proceedings of the VDI-Fachtagung Welle-Nabe-Verbindungen Gestaltung—Fertigung—Anwendungen, Stuttgart, Germany, 28 November 2016. [CrossRef]
19. Kröger, J.; Binz, H.; Wagner, M. Spannungsoptimierung von Pressverbindungen mit additiv gefertigten Naben—Numerische und experimentelle Untersuchungen. In Proceedings of the VDI-Fachtagung Welle-Nabe-Verbindungen Dimensionierung—Fertigung—Anwendung, Stuttgart, Germany, 26–27 November 2018. [CrossRef]